Rare Metal Materials and Engineering
Volume 51, Issue 5, May 2022
Available online at www.rmme.ac.cn

Science Press

Cite this article as: Lu Bingying, Ma Fei, Ma Dayan. Microstructure and Mechanical Properties of Thick Cr/CrN Multilayer Coatings by Multi-arc Ion Plating[J]. Rare Metal Materials and Engineering, 2022, 51(05): 1558-1564.

ARTICLE

Microstructure and Mechanical Properties of Thick Cr/CrN Multilayer Coatings by Multi-arc Ion Plating

Lu Bingying, Ma Fei, Ma Dayan

State Key Laboratory for Mechanical Behavior of Materials, Xi'an Jiaotong University, Xi'an 710049, China

Abstract: The thick Cr/CrN multilayer coatings with different modulation ratios (1:2, 1:3, 1:5) were deposited on the A100 steel substrate at room temperature by multi-arc ion plating (MAIP). The chamber temperature gradually rose to 160~170 °C during deposition. The modulation structures are designed to optimize the adhesion strength and the mechanical properties. The Cr/CrN multilayer coating with modulation ratio of 1:2 exhibits the highest adhesive strength (L_c=63.8 N), which may be attributed to the highest hardness (H)/elastic modules (E) and H^3/E^2 values of 0.083 and 0.138, respectively. The thicker the Cr layer, the better the plasticity and tribological properties. The dry friction test shows that the mean coefficient of friction and the specific wear rate of Cr/CrN multilayer coating are decreased by 24% and 94% at most, respectively, compared with those of the single-layer CrN coating. As the Cr layer becomes thick, the wear mechanism is transformed from surface fatigue wear to abrasive wear, which may be attributed to the coordinate changes of hardness and plasticity.

Key words: thick CrN coating; low-temperature deposition; coordination of mechanical properties; tribological performance

The transition metal nitrides (CrN and TiN) are widely used for surface protection of tools and molds due to their high hardness, excellent wear resistance, and good chemical stability[1-3]. However, there are a series of problems in monolayer nitride coatings, such as low adhesive strength and high brittleness[4]. The multilayer structures and nano-composite coatings can not only improve the adhesive strength of the coating, but also ameliorate their mechanical properties and corrosion resistance[5-7].

In multilayer systems, some transition metals, such as Cr, Ti, and Nb, are widely used as transition layers to improve the film toughness and film-substrate adhesive strength[8,9]. Compared to monolayer nitride coatings, the multilayer Cr/CrN and Ti/TiN coatings composed of alternative soft metal phases and hard ceramic phases show higher hardness, better wear resistance, and improved corrosion resistance[10,11]. The modulation ratio and modulation period of the composite structure are the key influencing parameters of composite performance. The appropriate modulation ratio and modulation period can provide the composite with excellent hardness, toughness, and tribological properties[12]. In addition, the interface also affects the mechanical and tribological properties of the multilayer composites by dissipating the fracture energy, changing the direction of crack propagation, and dividing the cracks into small cracks for further reaction with dislocations. Therefore, the interfaces can also enhance the tribological properties[11].

It is known that the modulation structure significantly affects the property of multilayer systems[12-14]. Xu et al[12] asserted that the low modulation ratio of TiAlN/ZrN is conducive to the formation of coherent interfaces and the alternating stress field formed by the coherent interface through first-principle energetics calculations, thereby improving the hardness of TiAlN/ZrN. Besides, the mechanical properties of nanoscale (Al, Cr)N/(Al, Cr)$_2$O$_3$ multilayer coatings also show the dependence on the modulation structure[15-17]. However, the regulation of the modulation structure of thin nitride films is mainly focused on the preparation of films with a thickness of several hundreds of nanometers to several micrometers at high temperature (250~550 °C)[18]. In this research, the thick Cr/CrN multilayer coatings with different modulation ratios were deposited at room temperature by multi-arc ion plating (MAIP), and their structure, morphology, mechanical properties, and friction

Received date: May 11, 2021
Corresponding author: Ma Dayan, Ph. D., Professor, State Key Laboratory for Mechanical Behavior of Materials, Xi'an Jiaotong University, Xi'an 710049, P. R. China, E-mail: madayan@mail.xjtu.edu.cn

performance were investigated. For comparison, the monolayer CrN coatings with the same thickness were also deposited. The chamber temperature rose from room temperature to 160~170 °C during the deposition. The Cr/CrN multilayer coatings with modulation ratio of 1:2 showed the optimal mechanical properties and friction performance. The optimum design for Cr/CrN multilayer system with appropriate mechanical properties at lower temperature (from room temperature to about 170 °C) was obtained.

1 Experiment

The Cr/CrN multilayer coatings were deposited by MAIP on polished A100 steel which is normally heat-treated until its hardness of 5.3 GPa is achieved. In this research, MAIP system was equipped with six sources of arc evaporation, as shown in Fig. 1. The specimens were placed on a rotating specimen holder after they were ultrasonically cleaned in ethanol for 15 min. The specimens were cleaned by glow discharge with substrate bias voltage of −800, −600, −400, and −200 V for 10 min to remove the adsorbents and oxides on the surface. The vacuum in the chamber was about 10^{-3} Pa before evaporation. The Ar gas flow of 1000 mL/min was used for the deposition of thin Cr interlayer from Cr targets using a current of 90 A and a bias voltage of −100 V for 10 min. The N_2 gas flow of 1300 mL/min was used to prepare the CrN layer. The target current was 100 A and the substrate bias voltage was 100 V. During the continuous growth of Cr/CrN multilayer coatings, the chamber temperature rose to 170 °C and the temperature deviation was less than ±10 °C. In this research, the specimens were deposited under the same modulation period to reach the same coating thickness with Cr/CrN modulation ratio of 1:2, 1:3, and 1:5, which were named as AC124, AC134, and AC154, respectively, as shown in Fig. 2. The single-layer CrN coatings named as AC001 were also deposited with the same thickness. The detailed deposition parameters are summarized in Table 1.

The thickness and cross-section microstructure of as-deposited coatings were observed by scanning electron

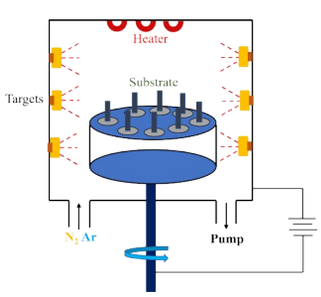

Fig.1 Schematic diagram of coating deposition setup

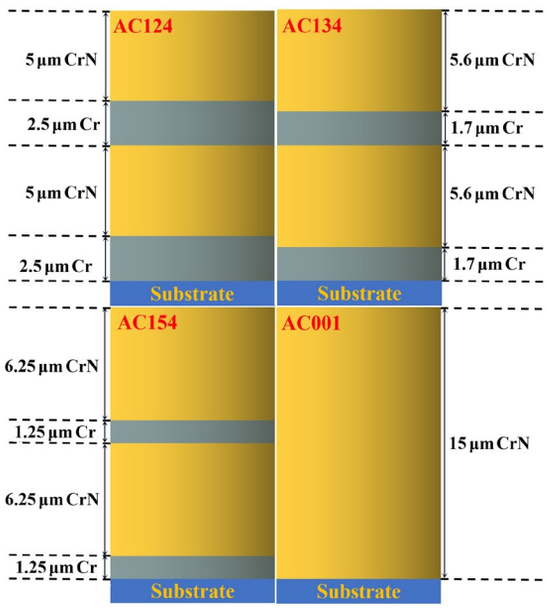

Fig.2 Schematic diagram of deposition coatings with different modulation structures

microscopy (SEM, ZEISS Gemini 500) equipped with energy dispersive spectrometry (EDS) analyzer (OXFORD X-Max). The X-ray diffractometer (XRD, Pert PRO) was used to identify the coating phase with a Cu Kα radiation (λ = 0.154 059 8 nm) at 40 kV and 30 mA under the scanning angle 2θ=30°~100° at 10°/min. The X-ray stress experiments were performed using the residual stress tester (MSF-M Japan).

The elastic modulus and hardness of the as-deposited coatings were measured using a TI950 TriboIndenter (Hysitrom, Minneapolis, MN) with a standard Berkovich tip. The mechanical test was performed using the load-controlled mode for all coatings at the strain rate of 0.1 s^{-1}. The elastic modulus and hardness were calculated by Oliver-Pharr method from the load-displacement curves. The WS2005 Instrument with a conical diamond tip of 0.2 mm in radius and 120° in taper angle was used to measure the adhesive strength of coatings and substrate during the scratch tests. The microstructure and morphologies of the scratch tracks were observed by optical microscopy (OM) to further analyze the coating failure. The anti-impact properties were tested by GP100K repeated impact testing machine with a WC ball of 2.5 mm in radius at the load of 300 N for 20 000 times.

The tribological test of as-deposited coatings was conducted using the ball-on-disc test tribometer (PCD-300A, Japan) under an air environment at room temperature of 20±3 °C. In addition, the Si_3N_4 ball with a diameter of 5 mm was selected as the counterpart. The wear test was conducted under a load of 2 N for 1000 m. The 3D optical profilometer

Table 1 Deposition parameters of Cr and CrN layers

Layer	Bias voltage/V	Target current/A	Partial pressure of N_2/Pa	Partial pressure of Ar/Pa	Deposition rate/μm·h^{-1}
Cr	−100	100	-	0.47	1.5
CrN	−100	100	1.3	-	5

(VK9700K, Japan) was used to observe the wear track morphology.

2 Result and Discussion

2.1 Microstructure and morphologies

Fig. 3 displays the cross-section morphologies of as-deposited coatings. The compact structure can be clearly observed in the terrace-like fracture surface. All the as-deposited coatings are well adhered to the substrate. In addition, no pinholes or pores can be observed. The total thickness is 15.7, 16.9, 16.7, and 16.7 μm for AC124, AC134, AC154, and AC001 coatings, respectively.

Fig. 4a shows XRD patterns of the monolayer coating and multilayer coatings. All coatings exhibit a typical Bl-NaCl face-centered cubic (fcc) structure with (111) orientation centered at 2θ=37.2° [19]. Unlike the random orientation of thin CrN films (thickness<4 μm) [20,21], the thick CrN coatings exhibit an obvious (111)-preferred orientation, which is related to the energy minimization theory[22]. According to the energy minimization theory, the coating energy depends on the strain energy and surface energy[23]. A large internal stress may be generated in the thick CrN coatings due to the substrate bias and ion bombardment. The CrN (111) plane is the most packed plane due to fcc structure. Thus, the strain energy of CrN (111) plane is the lowest. Therefore, the growth towards CrN (111) plane is conducive to the reduction in internal stress. Fig.4b shows that the CrN (111) peak position shifts of a small angle of about 0.3°, which is attributed to the high residual stress[24].

Besides, the Cr (110) and (200) (PDF 06-0694) diffraction peaks can be observed at 2θ =44.4° and 64.6° in the as-deposited multilayer coatings, respectively, indicating that the monolayer coating mainly contains CrN phase, and the multilayer coatings mainly contain CrN and Cr phases.

The residual stress of CrN coatings was measured by XRD (Smartlab) based on $\sin^2\psi$ method[25]. The interplanar distance d_{hkl} has a liner relationship with $\sin^2\psi$, and the measurement becomes more accurate as the characteristic peak becomes more obvious. Thus, the CrN (311) is chosen to be the characteristic peak, and the residual stress can be calculated by Eq.(1), as follows:

$$(d_{hkl} - d_0)/d_0 = \frac{1}{2}S_2\sigma\cos^2\alpha\sin^2\psi + \frac{1}{2}S_2\sigma\sin^2\alpha + 2S_1\alpha \quad (1)$$

where σ is the residual stress; d_0 is original interplanar spacing; S_1 and S_2 are constants related to Poisson's ratio v (about 0.2) and elastic modulus E (about 330 GPa), respectively; α is the angle related to the diffraction angle 2θ; ψ=0°, 15°, 30°, 45°. Then, Eq.(2) can be obtained, as follows:

$$\sigma = -\frac{E}{2(1+v)}\cot\theta_0\frac{\pi}{180}\frac{\partial 2\theta}{\partial\sin^2\psi} \quad (2)$$

Fig. 5 shows that 2θ has a good linear relationship with $\sin^2\psi$, indicating that the as-deposited AC124, AC134, AC154, and AC001 coatings are in the compressive stress state with stress of 6.48, 6.15, 6.54, and 7.96 GPa, respectively. Obviously, the residual stress of the multilayer coatings is much lower than that of the monolayer coating. Besides, the residual stress of the multilayer coatings with different modulation ratios is similar. There are two components attributed to the residual stress: the internal stress in CrN growth stage and the thermal stress caused by mismatched coefficient of thermal expansion between the coating and the substrate[25,26]. The monolayer CrN coatings grow for 4 h, but the relaxation mechanism does not play a key role in the residual stress. Relatively, Cr interfaces contribute to the reduced residual stress.

2.2 Mechanical properties

The hardness (H) and elastic modulus (E) of different

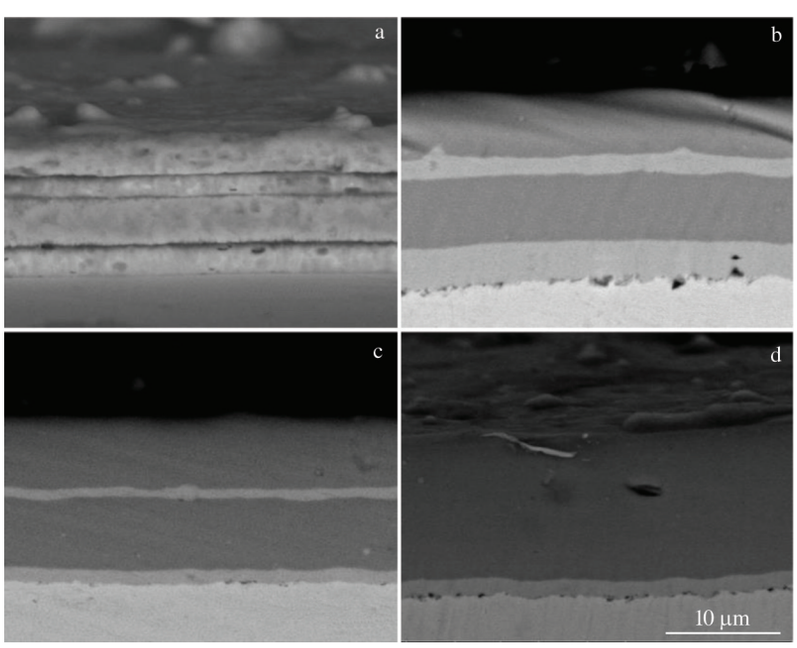

Fig.3 Cross-section morphologies of different as-deposited coatings: (a) AC124, (b) AC134, (c) AC154, and (d) AC001

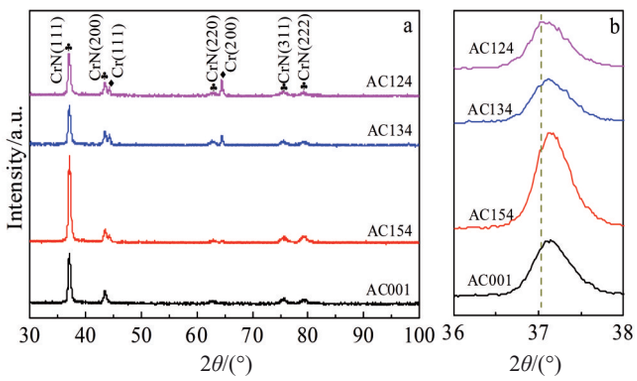

Fig.4 XRD patterns of different as-deposited coatings (a) and magnified XRD patterns around 2θ=37.2° (b)

coatings are shown in Table 2. The hardness of 17~20 GPa and elastic modulus of 241~256 GPa of the as-deposited CrN coating are similar to those of the multilayer coatings, which clearly demonstrates that the modulation structure of CrN coatings hardly affects the hardness and elastic modulus. In addition, the grain size of all as-deposited coatings is 21~24 nm. The similar hardness and elastic modulus of the coatings are mainly attributed to the classical Hall-Petch relationship[27,28]. The similar grain size indicates the similar hardness and elastic modulus. Besides, Oettel et al[29] proved that the influence of the compressive residual stress can be ignored by finite element method.

The values of H/E and H^3/E^2 were calculated to characterize the elastic strain failure resistance and plastic deformation resistance of the coatings, respectively. Joseph et al[30] pointed out that the improved wear resistance is attributed to the higher hardness and lower elastic modulus. Hence, the high H/E ratio means that the coating may have good elastic deformability for dynamic load resistance. In addition, the high H^3/E^2 value means that the coating has good resistance to crack initiation and propagation, which also implies the better wear resistance. Fig.6 shows the value of H/E and H^3/E^2 of all as-deposited coatings. AC124 coating has the highest H/E and H^3/E^2 of 0.083 and 0.138, respectively. H/E and H^3/E^2 of all coatings show the similar trends with decreasing the Cr modulation ratio. As Cr content decreases, H/E is gradually decreased from 0.083 to 0.069, and H^3/E^2 is decreased from 0.138 to 0.082. Moreover, the increased Cr modulation ratio shows a positive relationship with H/E and H^3/E^2.

The scratch test was performed to evaluate the adhesive strength between the substrate and the coatings. The high load-bearing capacity may indicate the excellent wear resistance.

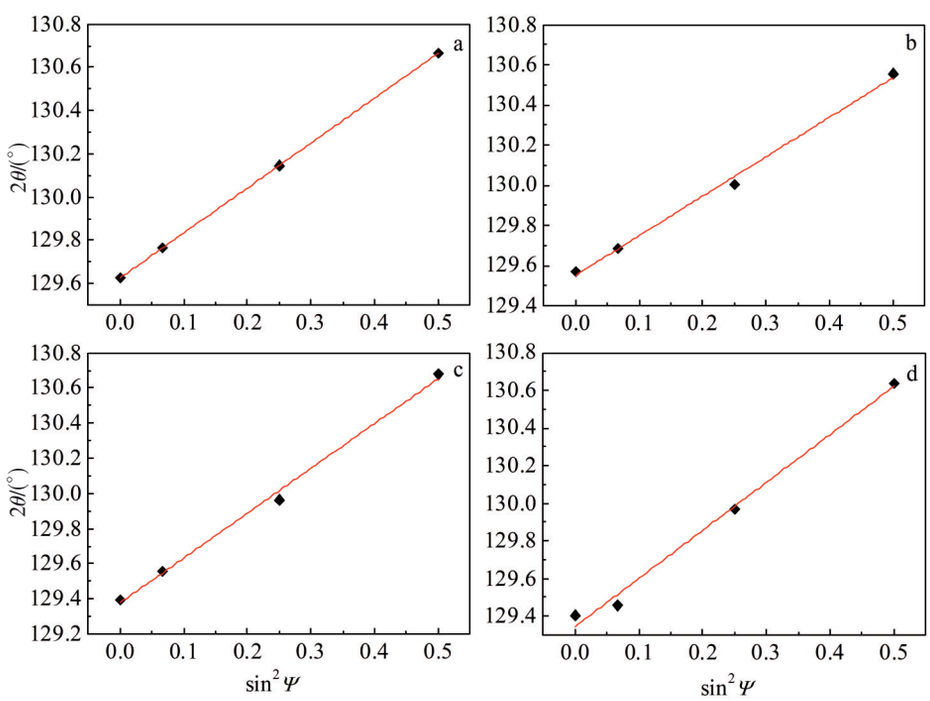

Fig.5 Relationship of 2θ-$\sin^2\psi$ of CrN (311) plane in different as-deposited coatings: (a) AC124, (b) AC134, (c) AC154, and (d) AC001

Table 2 Thickness, grain size, hardness, and elastic modulus of different as-deposited coatings

Coating	Modulation ratio	Thickness/μm	Grain size/nm	Hardness/GPa	Elastic modulus/GPa
AC124	1:2	15.7	21.26±0.19	20.02±1.88	241.10±15.49
AC134	1:3	16.9	21.26±0.24	19.48±4.12	256.07±42.97
AC154	1:5	16.7	24.08±0.24	18.90±2.41	247.10±15.34
AC001	-	16.5	21.41±0.27	17.00±0.31	244.58±13.73

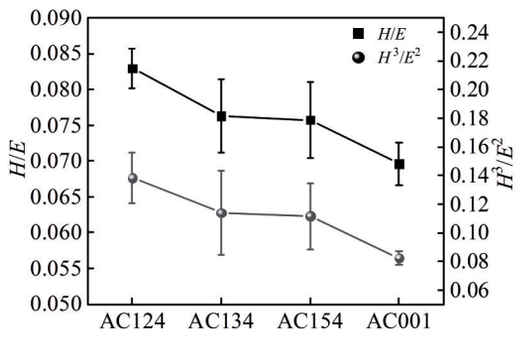

Fig.6 H/E and H^3/E^2 ratios of different as-deposited coatings

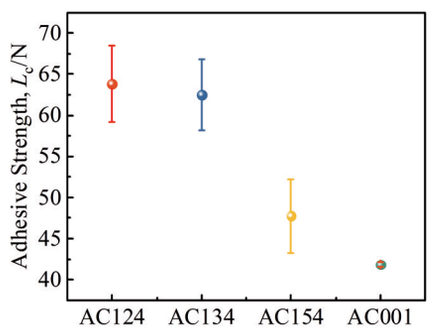

Fig.7 Adhesive strength L_c between different as-deposited coatings with substrate

Fig. 7 shows the adhesive strength of different as-deposited coatings. The AC124 specimen presents the highest load-bearing capacity (L_c=63.8 N) and optimal crack resistance. In addition, all the multilayer coatings exhibit much better load-bearing capacity than the monolayer coating does.

The multiple impact test was conducted to study the plastic deformation property of coatings. The stroke length was 1 mm and the frequency was 20 Hz. The surface morphologies were obtained by the 3D optical profilometer after the impact tests. Fig.8a shows the surface morphology of AC124 coating after impact test. The coating does not break and is still attached to the substrate, which indicates good plastic deformability. Fig. 8b and 8c show the similar morphologies of slightly broken coatings. As shown in Fig.8d, the spallation appears on the edge of the impact track on specimen surface, which may be attributed to the poor adhesive strength and inferior plastic deformability. It clearly demonstrates that the plastic deformation ability of the multilayer coatings is increased with increasing the Cr modulation ratio, therefore improving the wear resistance.

2.3 Tribological behavior

Fig. 9 presents the dry sliding coefficient of friction (COF) of all as-deposited coatings against the Si_3N_4 ball at room temperature. Compared with the multilayer coatings, COF of AC001 coating is suddenly increased from 0.6 to 0.73. As shown in Fig. 10, the wear tracks can be observed. The wear track depths of AC124, AC134, and AC154 coatings are 5.3, 13.5, and 15.3 μm, respectively, while the wear track depth of AC001 coating is 43 μm, indicating the poor tribological performance of AC001 coating.

The wear track width and depth are acquired using 3D optical profilometer. The wear loss volume is calculated by Eq.(3) and Eq.(4) [31], as follows:

$$W_V = \frac{t}{6b}(3t^2 + 4b^2) \times 2\pi r \quad (3)$$

$$W_S = \frac{W_V}{PS} \quad (4)$$

where W_v presents the wear loss volume; r is the radius of the wear track; t and b are the depth and width of the wear track, respectively; W_s is the specific wear rate; P is the load; S is the sliding distance.

Fig. 11 shows the specific wear rate and average COF of

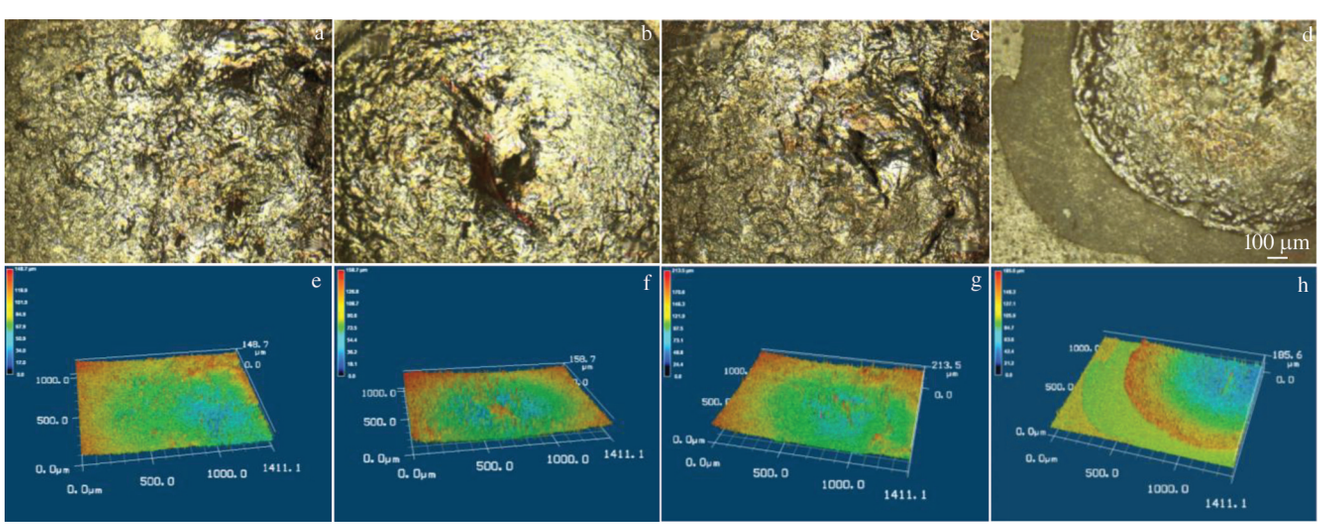

Fig.8 Actual (a~d) and simulated (e~f) surface morphologies of different as-deposited coatings after impact tests: (a, e) AC124, (b, f) AC134, (c, g) AC154, and (d, h) AC001

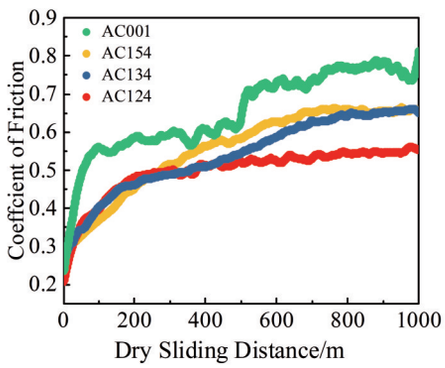

Fig.9 Dry sliding coefficient of friction of different as-deposited coatings

different as-deposited coatings. The AC001 coating shows the highest specific wear rate and average COF of 2.37×10^{-4} $mm^3\cdot N^{-1}\cdot m^{-1}$ and 0.654, respectively. The poor tribological properties can be attributed to the relatively low adhesive strength and poor resistance to elastic strain failure. As Cr modulation ratio increases, the specific wear rate and average COF is decreased from 2.37×10^{-4} $mm^3\cdot N^{-1}\cdot m^{-1}$ to 1.37×10^{-5} $mm^3\cdot N^{-1}\cdot m^{-1}$ and from 0.654 to 0.499, respectively. Compared with those of AC001 coating, the specific wear rate and average COF of multilayer coatings are decreased by 24% and 94%, respectively. As shown in Fig.12, SEM images of wear track are acquired to further investigate the wear failure mechanism. The wear surface of AC124 coating has many continuous furrows parallel to the sliding direction, which

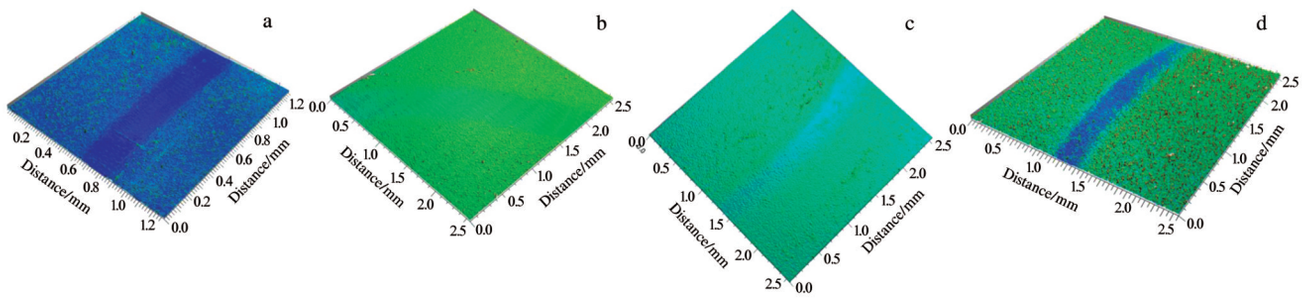

Fig.10 Morphologies of wear tracks on different as-deposited coatings: (a) AC124, (b) AC134, (c) AC154, and (d) AC001

indicates a typical abrasive wear mechanism. Due to the relatively low hardness, the wear debris is rolled and fragmented as the third-body interface during the friction test. The softer third-body debris can act as the buffer layer to participate in the interface behavior, which promotes the wear resistance of AC124 coating. As Cr content increases, the typical furrows parallel to the sliding direction gradually disappear, which is attributed to the decreased hardness. Moreover, the pitting is distributed on the wear surface of AC134 and AC154 coatings, which indicates that the wear mechanism is transformed to the surface fatigue wear. The wear mechanism of AC001 coating is also surface fatigue wear, but the failure form is transformed from pitting to flaky spallation. Beagley[32] proved the transition from pitting to flaky spallation by the delamination theory of wear.

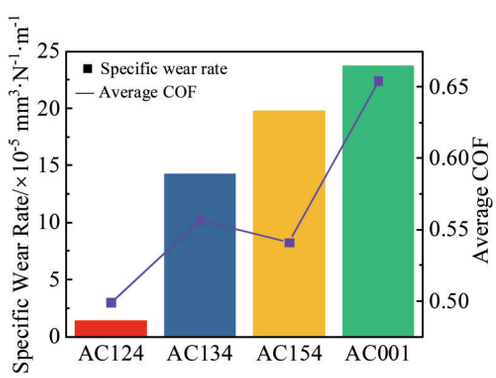

Fig.11 Average coefficient of friction (COF) and specific wear rate of different as-deposited coatings against Si_3N_4 balls at room temperature

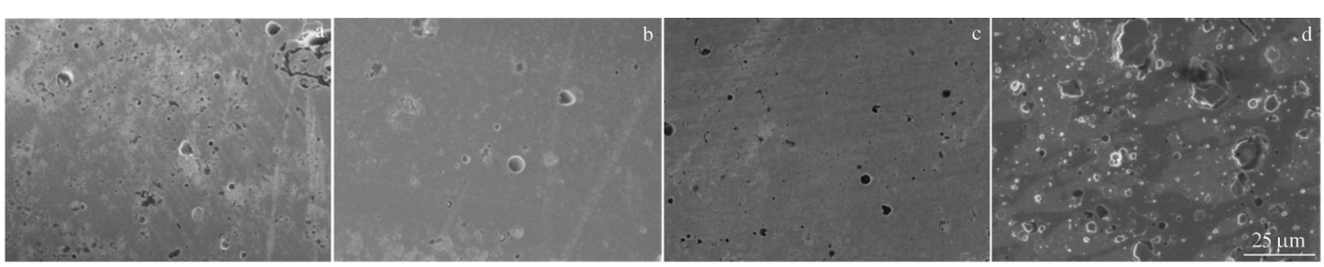

Fig.12 SEM microstructures of wear track of different as-deposited coatings at room temperature: (a) AC124, (b) AC134, (c) AC154, and (d) AC001

3 Conclusions

1) Because all the as-deposited coatings obey the Hall-Petch relationship, the multilayer Cr/CrN coatings and monolayer CrN coating exhibit the similar hardness of 17~20 GPa and elastic modulus of 241~256 GPa.

2) The multilayer Cr/CrN coatings show good cohesive strength and plastic deformation ability, which is mainly attributed to the increase in the ratios of hardness (H)/elastic modules (E) and H^3/E^2. Moreover, the increased Cr modulation ratio shows a positive relationship with H/E and H^3/E^2.

3) The multilayer Cr/CrN coatings show excellent wear resistance. As Cr modulation ratio increases, the wear mechanism is changed from surface fatigue wear to abrasive wear, which can be attributed to the higher hardness and better plastic deformation ability.

4) This simple preparation of thick Cr/CrN multilayer coatings with high adhesive strength, low coefficient of friction, and good wear resistance at relatively low temperature is beneficial for commercial and industrial applications.

References

1 Bagcivan N, Bobzin K, Ludwig A *et al*. *Thin Solid Films*[J], 2014, 572: 153
2 Delisle D A, Krzanowski J E. *Thin Solid Films*[J], 2012, 524: 100
3 Lotfi-Khojasteh E, Sahebazamani M, Elmkhah H *et al*. *Journal of Asian Ceramic Societies*[J], 2020, 9(1): 247
4 Ibrahim R N, Rahmat M A, Oskouei R H *et al*. *Engineering Fracture Mechanics*[J], 2015, 137: 64
5 Liu S Y, Yang Y, Ji R *et al*. *Scripta Materialia*[J], 2017, 130: 242
6 Manimunda P, Al-Azizi A, Kim S H *et al*. *ACS Applied Materials & Interfaces*[J], 2017, 9(19): 16 704
7 Wan Z X, Zhang T F, Lee H B R *et al*. *ACS Applied Materials & Interfaces*[J], 2015, 7(48): 26 716
8 Sui X D, Li G J, Jiang C J *et al*. *Ceramics International*[J], 2018, 44(5): 5629
9 Adesina A Y, Gasem Z M, Mohammed A S. *Arabian Journal for Science and Engineering*[J], 2019, 44(12): 10 355
10 Guan X Y, Wang Y X, Xue Q J *et al*. *Surface and Coatings Technology*[J], 2015, 282: 78
11 Meindlhumer M, Brandt L R, Zalesak J *et al*. *Materials & Design*[J], 2021, 198: 109 365
12 Xu Y X, Chen L, Pei F *et al*. *Acta Materialia*[J], 2017, 130: 281
13 Tang J F, Huang C H, Lin C Y *et al*. *Surface and Coatings Technology*[J], 2019, 379: 125 051
14 Liu H, Yang F C, Tsai Y J *et al*. *Surface and Coatings Technology* [J], 2019, 358: 577
15 Ho W Y, Huang D H, Huang L T *et al*. *Surface and Coatings Technology*[J], 2004, 177-178: 172
16 Hsu C H, Huang D H, Ho W Y *et al*. *Materials Science and Engineering A*[J], 2006, 429(1-2): 212
17 Wang D Y, Chiu M C. *Surface and Coatings Technology*[J], 2001, 137(2-3): 164
18 Gao B, Du X Y, Li Y H *et al*. *Journal of Alloys and Compounds* [J], 2019, 797: 1
19 Suzuki K, Kaneko T, Yoshida H *et al*. *Journal of Alloys and Compounds*[J], 1995, 224(2): 232
20 Chou T L, Yang S Y, Chiang K N. *Thin Solid Films*[J], 2011, 519(22): 7883
21 Pedrosa P, Rodrigues M S, Neto M A *et al*. *Surface and Coatings Technology*[J], 2018, 349: 858
22 Oh U C, Je J H, Lee J Y. *Journal of Materials Research*[J], 1998, 13(5): 1225
23 Zhao Z B, Rek Z U, Yalisove S M *et al*. *Surface and Coatings Technology*[J], 2004, 185(2-3): 329
24 Li Z C, Wang Y X, Cheng X Y *et al*. *ACS Applied Materials & Interfaces*[J], 2018, 10(3): 2965
25 Fan D, Lei H, Guo C Q *et al*. *Acta Metallurgica Sinica* (*English Letters*)[J], 2017, 31(3): 329
26 Chen X, Pang X L, Meng J *et al*. *Ceramics International*[J], 2018, 44(6): 5874
27 Lee K, Kang N, Bae J S *et al*. *Metals and Materials International* [J], 2016, 22(5): 842
28 Hu J, Shi Y N, Sauvage X *et al*. *Science*[J], 2017, 355(6331): 1292
29 Oettel H, Wiedemann R. *Surface and Coatings Technology*[J], 1995, 76-77: 265
30 Joseph M C, Tsotsos C, Baker M A *et al*. *Surface and Coatings Technology*[J], 2005, 190(2-3): 345
31 Wang J L, Jia Q, Yuan X Y *et al*. *Applied Surface Science*[J], 2012, 258(24): 9531
32 Beagley T M. *Wear*[J], 1978, 47(2): 417

多弧离子镀制备Cr/CrN多层厚膜的微观结构和力学性能

卢丙迎，马　飞，马大衍

(西安交通大学 金属材料强度国家重点实验室，陕西 西安 710049)

摘　要：通过多弧离子镀（MAIP）在室温下将具有不同调制比（1:2、1:3、1:5）的多层Cr/CrN厚涂层沉积在A100钢基底上。腔室温度在沉积过程中由室温逐渐升高到160~170 ℃。设计调制结构是为了使膜/基结合强度和机械性能最大化。调制比为1:2的Cr/CrN多层涂层表现出最高的膜/基结合强度（L_c=63.8 N），这可能归因于最高的材料硬度(H)/弹性模量(E)和H^3/E^2数值比（分别为0.083和0.138）。Cr层越厚，多层Cr/CrN厚涂层的塑性和摩擦学性能越好。干摩擦试验表明，与单层CrN相比，Cr/CrN多层涂层的平均摩擦系数和比磨损率分别最高降低了24%和94%。随着Cr层变厚，磨损机理从表面疲劳磨损转变为磨料磨损，这种现象可归因于硬度和塑性的协调变化。

关键词：CrN厚涂层；低温沉积；力学性能调控；摩擦性能

作者简介：卢丙迎，男，1995年生，硕士，西安交通大学金属材料强度国家重点实验室，陕西 西安 710049，E-mail：lubingying@stu.xjtu.edu.cn